

# Slow Inactivation of a TEA-Sensitive K Current in Acutely Isolated Rat Thalamic Relay Neurons

J. R. HUGUENARD AND D. A. PRINCE

*Department of Neurology and Neurological Sciences, Stanford University School of Medicine, Stanford, California 94305*

## SUMMARY AND CONCLUSIONS

1. Voltage-gated K currents were studied in relay neurons (RNs) acutely isolated from somatosensory (VB) thalamus of 7- to 14-day-old rats. In addition to a rapidly activated, transient outward current,  $I_A$ , depolarizations activated slower  $K^+$  currents, which were isolated through the use of appropriate ionic and pharmacological conditions and measured via whole-cell voltage-clamp.

2. At least two slow components of outward current were observed, both of which were sensitive to changes in  $[K^+]_o$ , as expected for K conductances. The first,  $I_{K1}$ , had an amplitude that was insensitive to holding potential and a relatively small conductance of 150 pS/pF. It was blocked by submillimolar levels of tetraethylammonium [TEA, 50%-inhibitory concentration ( $IC_{50} = 30 \mu M$ )] and 4-aminopyridine (4-AP, 40  $\mu M$ ). In the absence of intracellular  $Ca^{2+}$  buffering, the amplitude of  $I_{K1}$  was both larger and dependent on holding potential, as expected for a  $Ca^{2+}$ -dependent current. Replacement of  $[Ca^{2+}]_o$  by  $Co^{2+}$  reduced  $I_{K1}$ , although the addition of  $Cd^{2+}$  to  $Ca^{2+}$ -containing solutions had no effect.

3. The second component,  $I_{K2}$ , had a normalized conductance of 2.0 nS/pF and was blocked by millimolar concentrations of TEA ( $IC_{50} = 4 mM$ ) but not by 4AP. The kinetics of  $I_{K2}$  were analogous to (but much slower than) those of  $I_A$  in that both currents displayed voltage-dependent activation and voltage-independent inactivation.  $I_{K2}$  was not reduced by the addition of  $Cd^{2+}$  to  $Ca^{2+}$ -containing solutions or by replacement of  $Ca^{2+}$  by  $Co^{2+}$ .

4.  $I_{K2}$  had a more depolarized activation threshold than  $I_A$  and attained peak amplitude with a latency of  $\sim 100$  ms at room temperature.  $I_{K2}$  decay was nonexponential and could be described as the sum of two components with time constants ( $\tau$ ) near 1 and 10 s.

5.  $I_{K2}$  was one-half steady-state inactivated at a membrane potential of  $-63$  mV, near the normal resting potential for these cells. The slope factor of the Boltzmann function describing steady-state inactivation was  $13 mV^{-1}$ , which indicates that  $I_{K2}$  varies in availability across a broad voltage range between  $-100$  and  $-20$  mV.

6. Activation kinetics of  $I_{K2}$  were voltage dependent, with peak latency shifting from 300 to 50 ms in the voltage range  $-50$  to  $+30$  mV. Deactivation and reactivation were also voltage dependent, in contrast to inactivation, which showed little dependence on membrane potential. Increase in temperature sped the kinetics of  $I_{K2}$ , with temperature coefficient ( $Q_{10}$ ) values near 3 for activation and inactivation. Heating increased the amplitude of  $I_{K2}$  with a  $Q_{10}$  value near 2.

7. Prolonged near-threshold depolarizing stimuli in RNs can activate  $I_{K2}$ , which initially inhibits spike firing. However, maintained stimulation will cause inactivation of  $I_{K2}$ , with an accompanying gradual depolarization that can eventually reach spike threshold. Therefore one function of  $I_{K2}$  may be to cause delayed and/or accelerating spike firing in response to sustained depolarizing stimuli, allowing RNs to alter their integrating response to afferent inputs over periods of several seconds.

## INTRODUCTION

Regulation of action potential firing frequency in neurons is an important factor contributing to behavior (Llinás 1988; Steriade and Llinás 1988). In cells of the thalamus, two general patterns are observed, one of sustained regular firing and another involving generation of high-frequency bursts of action potentials (Deschênes et al. 1982; Llinás and Jahnsen 1982). In general, burst-firing patterns are associated with periods of drowsiness and slow-wave sleep, whereas regular firing is seen during arousal or rapid eye movement (REM) sleep (reviewed by Steriade and Llinás 1988). In addition, there is a growing body of evidence that burst firing may also be associated with petit mal epilepsy (Buzsáki et al. 1990; Coulter et al. 1989b; Gloor and Fariello 1988; Vergnes et al. 1990) and that some anticonvulsant drugs may exert their action by inhibiting the generation of thalamic burst rhythms (Coulter et al. 1989b, 1990).

The importance of a prominent transient  $Ca^{2+}$  current (T current or  $I_T$ ) for burst-firing modes in the relay neurons (RNs) of the thalamus has been previously elaborated in current-clamp (Deschênes et al. 1982; Jahnsen and Llinás 1984) and voltage-clamp recordings (Coulter et al. 1989a; Hernández-Cruz and Pape 1989; Suzuki and Rogawski 1989; Crunelli et al. 1989). To more completely understand such cellular rhythms it is important to examine other factors, both intrinsic and extrinsic, that interact with the T current to affect RN firing patterns. We have recently characterized the fast transient  $K^+$  current ( $I_A$ ) current in these cells and have shown that it contributes to at least three cellular phenomena in the thalamus (Huguenard et al. 1991). 1) As hypothesized for other types of neurons (Connor and Stevens 1971b; Segal et al. 1984),  $I_A$  increases the dynamic range of firing rates that occur in response to stimulation by allowing slow-frequency firing to occur with small depolarizations. 2)  $I_A$  activation is rapid enough to contribute to  $Na^+$  spike repolarization. 3) Because the time course of  $I_A$  is similar to that of  $I_T$ , it may be one factor that controls burst generation.

Although  $I_A$  and  $I_T$  are important in regulating firing behavior in RNs, their kinetics are too rapid to allow these currents to have functional roles in integrating the ongoing tonic synaptic excitation that RNs receive through various sensory pathways. Other outward currents with slower kinetics of activation and inactivation appear to be important in this role. Such slow currents make a large contribution to overall  $K^+$  conductances in RNs. Although their amplitudes are smaller than  $I_A$ , they can be quite influential in shaping RN output. The experiments reported here focus

on an analysis of these currents and their functions in RNs. A preliminary report has been published in abstract form (Huguenard et al. 1990).

## METHODS

Methods were essentially the same as previously described (Huguenard et al. 1991). Briefly, RNs were acutely isolated from the somatosensory (VB) complex of 7- to 15-day-old Sprague-Dawley rats using a modification of the technique described by Kay and Wong (1986). Brains were obtained from pentobarbital sodium-anesthetized animals, and coronal slices (500  $\mu$ m thick) were cut on a vibratome. Those slices containing VB were incubated for 45–90 min in oxygenated PIPES buffered saline containing trypsin (Type XI, 8 mg/10 ml), then rinsed in enzyme-free solution. The VB complex was excised from each slice and triturated with fire-polished Pasteur pipettes, resulting in cell suspensions that were plated onto 35-mm plastic petri dishes. PIPES-buffered saline consisted of (in mM) 120 NaCl, 5 KCl, 1 MgCl<sub>2</sub>, 1 CaCl<sub>2</sub>, 25 glucose, and 20 piperazine-*N,N'*-bis[2-ethanesulfonic acid] (PIPES); the pH was adjusted to 7.0 with NaOH (Kay and Wong 1986). The intracellular solution was as follows (in mM): 130 KCl, 10 *N*-2-hydroxyethylpiperazine-*N'*-2-ethanesulfonic acid (HEPES), 11 ethylene glycol-bis( $\beta$ -aminoethyl ether)-tetraacetic acid (EGTA), 1 MgCl<sub>2</sub>, 1 CaCl<sub>2</sub>, 4 Na<sub>2</sub>ATP, 22 phosphocreatine, and 50 U/ml creatinine phosphokinase, pH 7.3. Osmolality of both intracellular and extracellular solutions was adjusted to 305 mosmol/kg H<sub>2</sub>O before each experiment. The extracellular recording solution consisted of (in mM) 155 NaCl, 3 KCl, 1 MgCl<sub>2</sub>, 1 CaCl<sub>2</sub>, 0.0005 tetrodotoxin (TTX), and 10 HEPES with pH ad-

justed to 7.4. This level (1 mM) of extracellular Ca<sup>2+</sup> maximized cell viability while minimizing calcium current (*I*<sub>Ca</sub>; Huguenard et al. 1991). Inorganic blockers of Ca<sup>2+</sup> current (e.g., Cd<sup>2+</sup> or La<sup>3+</sup>) were not used because these produced large shifts in the voltage-dependent activation and inactivation of potassium currents (*I*<sub>K</sub>; Huguenard et al. 1991; Mayer and Sugiyama 1988). In one group of experiments, K-gluconate was substituted on an equimolar basis for KCl in the intracellular solution. The liquid junction potential measured in the bath by the method of Hagiwara and Ohmori (1982) for electrodes containing the K-gluconate solution was large (9 mV). Because the electrode potential was nulled in the bath, the membrane potential was obtained by subtracting the liquid junction potential from the command potential. All chemicals were obtained from Sigma (St. Louis, MO). MCD peptide was obtained from Latoxan (Rosans, France). TEA-Cl was substituted on an equimolar basis for NaCl. Solution changes were made using the sewer pipe method as previously described (Huguenard et al. 1991). In experiments in which extracellular K<sup>+</sup> concentrations ([K<sup>+</sup>]<sub>o</sub>) were varied, KCl was substituted on an equimolar basis for NaCl.

Whole-cell voltage-clamp recordings (Hamill et al. 1981) were obtained with a List EPC-7 amplifier (Medical Systems) employing series resistance compensation. Patch electrodes were pulled from borosilicate glass (Garner Glass, Claremont, CA; KG-33, 1.8-mm OD, 1.3-mm ID) and, when filled with KCl, measured 2–3 M $\Omega$  in the bath. Methods based on those of Blanton et al. (1989) and Otis et al. (1991) were used to obtain whole-cell recordings (e.g., Fig. 1) in 400- $\mu$ M brain slices containing the VB complex. Slices were maintained at 32°C in an interface chamber and superfused with oxygenated, bicarbonate-buffered saline contain-

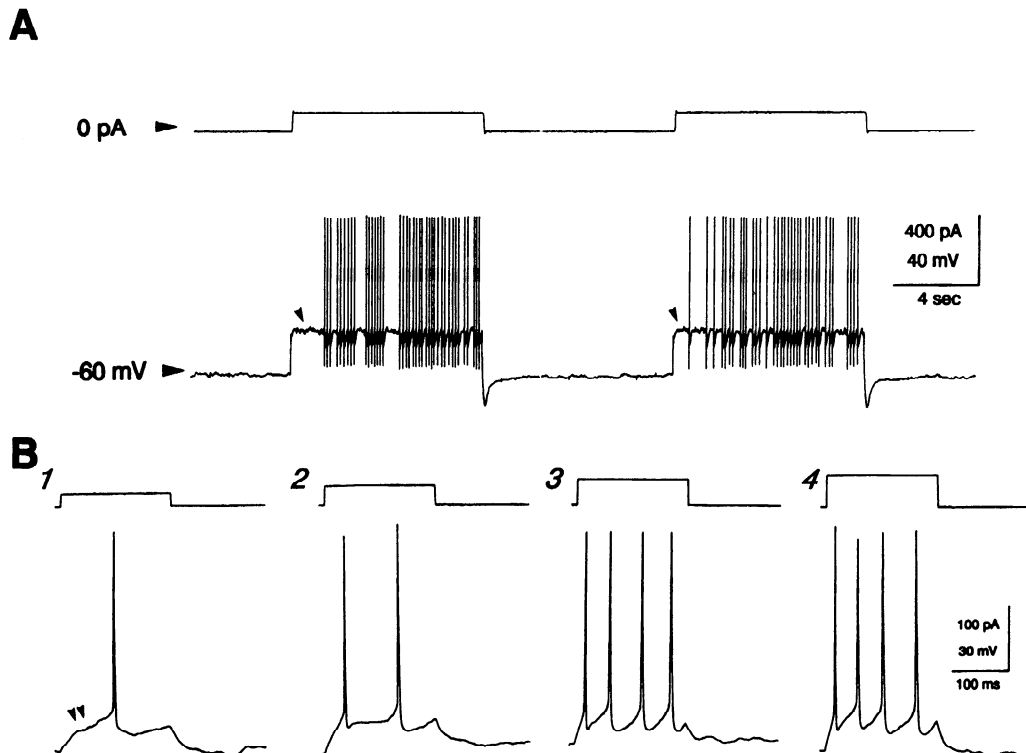


FIG. 1. Intracellular voltage recordings made with patch-clamp electrodes in slices (*A*) and in acutely isolated VB relay neurons (*B*). *A*: in slice-patch recordings, small depolarizing current steps result in repetitive firing, but only after significant delays ( $\blacktriangle$ ) of 0.5–1.5 s. A holding current of  $-30$  pA was applied to hyperpolarize the cell to  $-62$  mV, then 10-s depolarizing commands of  $+130$  pA were applied every 20 s. *B*: depolarizing current pulses produce repetitive firing in isolated RNs bathed in extracellular solution devoid of TTX. Action potentials with apparently normal morphology are evoked in increasing number as the stimulation strength is increased. Note the slight delay in latency to 1st spike for threshold depolarization ( $\blacktriangle$  in *B1*). Holding current was  $-110$  pA. Stimulation currents were  $+20$ ,  $+30$ ,  $+40$ , and  $+50$  pA in *B1*–*B4*, respectively, whereas corresponding resting membrane potentials were  $-64$ ,  $-67$ ,  $-62$ , and  $-64$  mV.

ing (in mM) 126 NaCl, 26 NaHCO<sub>3</sub>, 2.5 KCl, 1.25 NaH<sub>2</sub>PO<sub>4</sub>, 2 MgCl<sub>2</sub>, 2 CaCl<sub>2</sub>, and 10 glucose). The pipette solution was the normal KCl intracellular solution, minus ATP, CPK, and creatinine phosphate.

## RESULTS

### Possible functions for outward K<sup>+</sup> currents in RNs

Typical patch-electrode current-clamp recordings from a neuron in the VB complex, obtained from a brain slice maintained at 32°C *in vitro*, are shown in Fig. 1*A*. Weak depolarizations, which appeared to be subthreshold for up to several seconds after the onset of the current pulse (▲ in Fig. 1*A* voltage trace), would subsequently result in repetitive firing. This delay to the onset of spike generation is much too long to be accounted for by inactivation of *I<sub>A</sub>* (Huguenard et al. 1991) and must be due to underlying currents that have slower kinetics. In the experiment of Fig. 1*A*, it is not possible to distinguish between an underlying slow activation of inward current and inactivation of outward current to explain the firing behavior. If a K current, its kinetics are likely to be similar to those found in a variety of neurons, including those in guinea pig (Jahnsen and Llinás 1984) and cat thalamus (McCormick 1990), vagal

motor nucleus (Laiwand et al. 1988), hippocampus (Storm 1988), inferior olive (Yarom and Llinás 1987), and the histaminergic cells of hypothalamus (Greene et al. 1990). When activated by near-threshold depolarizations, this current can cause a significant delay (1–10 s) before spike threshold is reached. The delay appears to be due to outward current inactivation, which results in a net depolarization that eventually causes the membrane potential to reach firing threshold.

Because the acutely isolated neurons to be used in this voltage-clamp study had undergone some changes, including marked truncation of dendritic and axonal processes, and had been exposed to a proteolytic enzyme, we obtained current-clamp recordings to determine whether there were obvious alterations in electrical properties. As can be seen in Fig. 1*B*, these neurons were capable of firing both single and repetitive action potentials when in TTX-free saline, indicating that their basic action potential depolarization and repolarization mechanisms were intact. With threshold depolarizations, a delay to first spike was observed (Fig. 1*B1*, ▲▲), probably due to activation of *I<sub>A</sub>*. Because these neurons in isolation do not have very stable resting potentials (–62 to –67 mV in Fig. 1*B*), it proved impractical to demonstrate the type of long delay shown in Fig. 1*A*. Never-

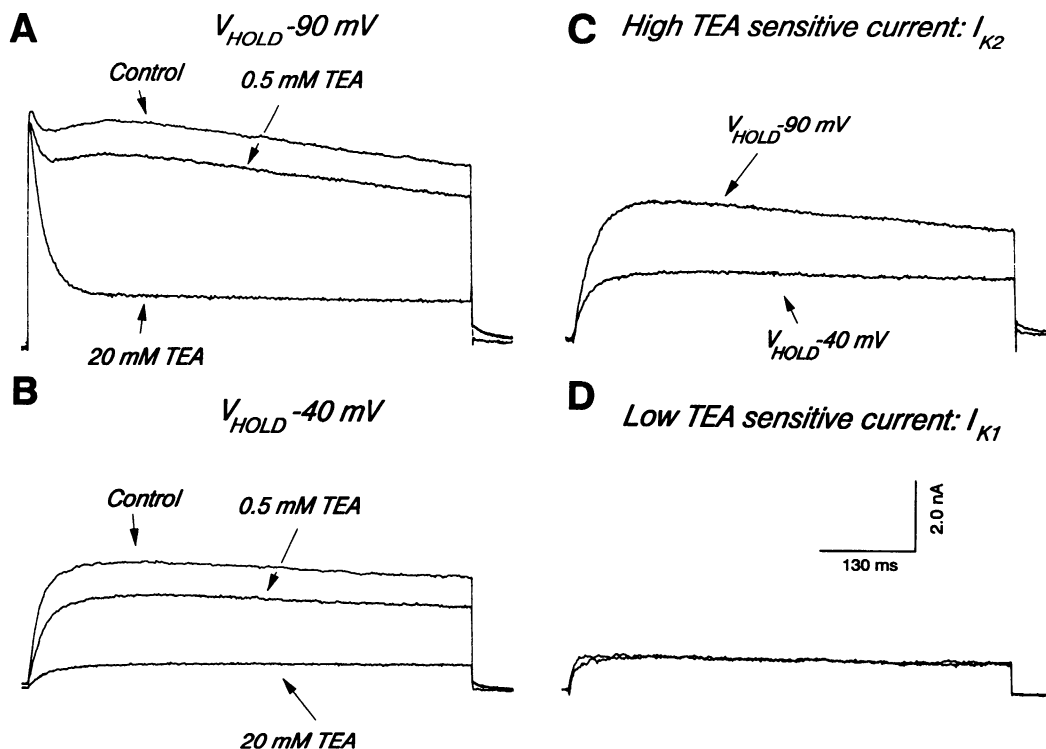


FIG. 2. Two long-lasting K<sup>+</sup> currents in RNs. *A*: long depolarizations (600 ms) to 0 mV from a holding potential of –90 mV were applied every 10 s. These commands were alternated with those with the holding potential set to –40 mV (*B*). Addition of 0.5 mM TEA to the bath resulted in the blockade of a small fraction of total outward current (compare control and 0.5 mM TEA traces). When TEA concentration was raised to 20 mM, a much larger amount of current was blocked, leaving mainly *I<sub>A</sub>* (compare control and 20 mM TEA traces). *B*: with reduced  $V_{\text{hold}}$ , 0.5 mM TEA blocks the same absolute current amount as it does at hyperpolarized  $V_{\text{hold}}$  in *A*, but the relative current block in *B* (27%) with reduced  $V_{\text{hold}}$  is greater than that in *A* (14%). High (20 mM) TEA blocks most of the remaining current. *C*: current blocked by high TEA at the 2  $V_{\text{hold}}$ s is obtained by subtracting currents obtained with 20 mM TEA from those obtained with 0.5 mM TEA in *A* and *B*. This current, *I<sub>K2</sub>*, is steady-state inactivated by changes in  $V_{\text{hold}}$  (note difference in current amplitudes) and relatively slow in rate of activation and deactivation. *D*: net submillimolar-TEA-sensitive current (*I<sub>K1</sub>*) is obtained by subtracting control from 0.5 mM TEA traces in *A* and *B*. This current is not steady-state inactivated and is relatively fast in activation and deactivation kinetics.

theless, we can conclude that the K<sup>+</sup> currents, which are necessary to 1) repolarize action potentials and 2) promote repetitive firing, are not significantly affected in RNs by the dissociation procedure.

#### Two depolarization-activated, long-lasting K<sup>+</sup> currents in RNs

In isolated RNs, voltage-clamp depolarizations evoked relatively persistent outward K<sup>+</sup> currents made up of at least two components (Huguenard et al. 1991), which are illustrated in Fig. 2. The first component, I<sub>K1</sub>, was selectively blocked by low concentrations of TEA [50%-inhibitory concentration (IC<sub>50</sub>) = 30–40 μM]. When the holding potential was set to -90 mV, the current blocked by 0.5 mM TEA was relatively time invariant (Fig. 2*A*); i.e., the amplitude of blocked current remained the same throughout the depolarization (Fig. 2*D*). In contrast, higher concentrations of TEA (20 mM) blocked a current, I<sub>K2</sub>, that activated gradually over several tens of milliseconds and then began to slowly inactivate (Fig. 2*C*). I<sub>K1</sub> was relatively independent of holding potential and deactivated rapidly on termination of the depolarizing command, as seen by the lack of slow tail current (Fig. 2*D*). I<sub>K2</sub> varied in amplitude with changes in holding potential (Fig. 2*C*) and deactivated rather slowly (see tail currents). All effects of external TEA were rapidly and completely reversible.

The voltage-dependent properties of I<sub>K2</sub>, combined with its millimolar TEA sensitivity, are similar to those expected for a delayed rectifier current (Hodgkin and Huxley 1952; Sah et al. 1988; Segal and Barker 1984). Even the property of slow inactivation (Clay 1989) is similar to that seen in invertebrate axons. Therefore I<sub>K2</sub> may be analogous to the delayed rectifier. Because the inactivation of such a current can have an influence on the long-term excitability of relay neurons over seconds, we further characterized the voltage-dependent kinetic properties of I<sub>K2</sub> within a Hodgkin-Huxley framework.

The time course of I<sub>K2</sub>, obtained as the current blocked by 20 mM TEA, is shown in Fig. 3. With these long depolarizations (1 s in Fig. 3, *A–C*), the partial inactivation of late outward current can clearly be seen (see also Fig. 7). In addition, peak amplitude was attained with shorter latency as the depolarization was increased (Fig. 3*D* and arrowheads in *A* and *C*). Because peak latency is affected by both activation and inactivation rates and the rate of inactivation of I<sub>K2</sub> is largely independent of voltage (see Fig. 7), the shift in peak latency is mostly due to a voltage-dependent activation rate (Fig. 4*D*). The time course of I<sub>K1</sub> was somewhat more difficult to assess, because the current obtained by subtraction was small compared with the total current and relatively minor changes in total current amplitude could therefore have nontrivial effects. Nonetheless, from

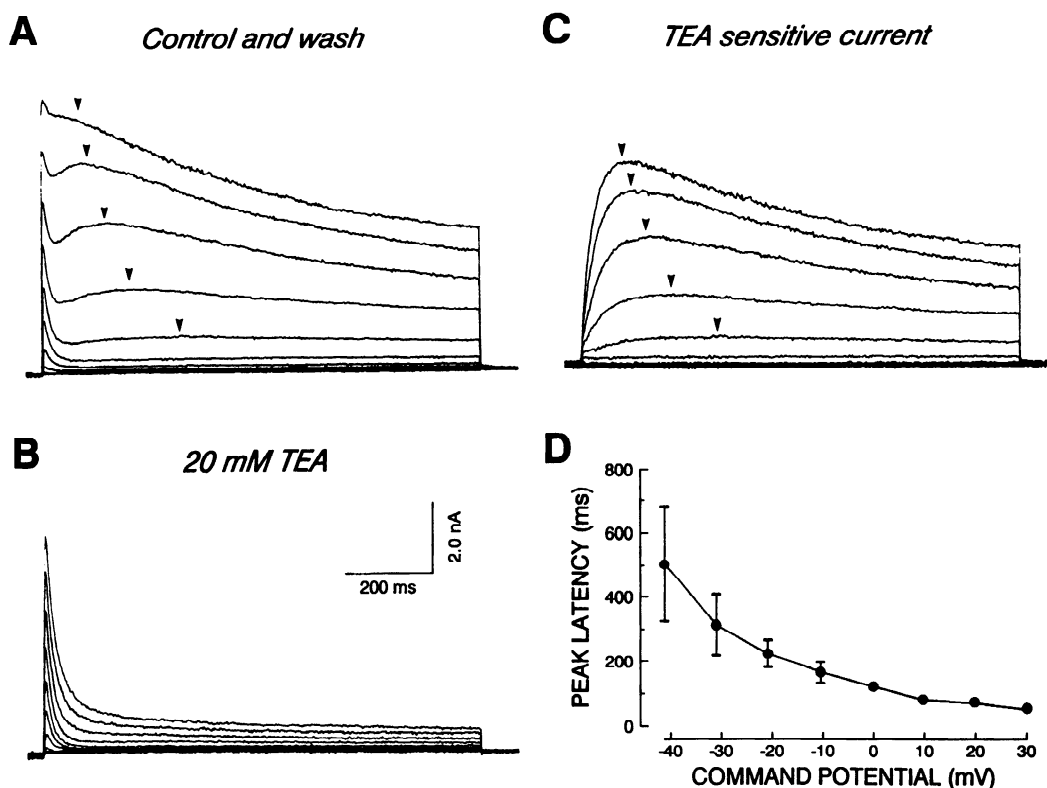


FIG. 3. Rate of I<sub>K2</sub> activation is voltage dependent. *A*: each trace is average of 1 control (pre-TEA) and 1 wash (post-TEA) current at each voltage. Currents were evoked by long (1 s) depolarizations to potentials between -70 and +20 mV in steps of 10 mV. Arrowheads indicate the appearance of a 2nd outward current peak, which occurred with considerable latency after the early transient outward current, I<sub>A</sub>. *B*: in the presence of high TEA, the late-peaking outward current was nearly completely blocked. *C*: millimolar-TEA-sensitive current was obtained by subtraction of the currents in *A* and *B*. Arrowheads indicate peak latency, which became shorter with increasing depolarizations. *D*: peak latency curve for TEA-sensitive current. Each point is the average of 4–6 cells, and error bars represent ±1 SE.

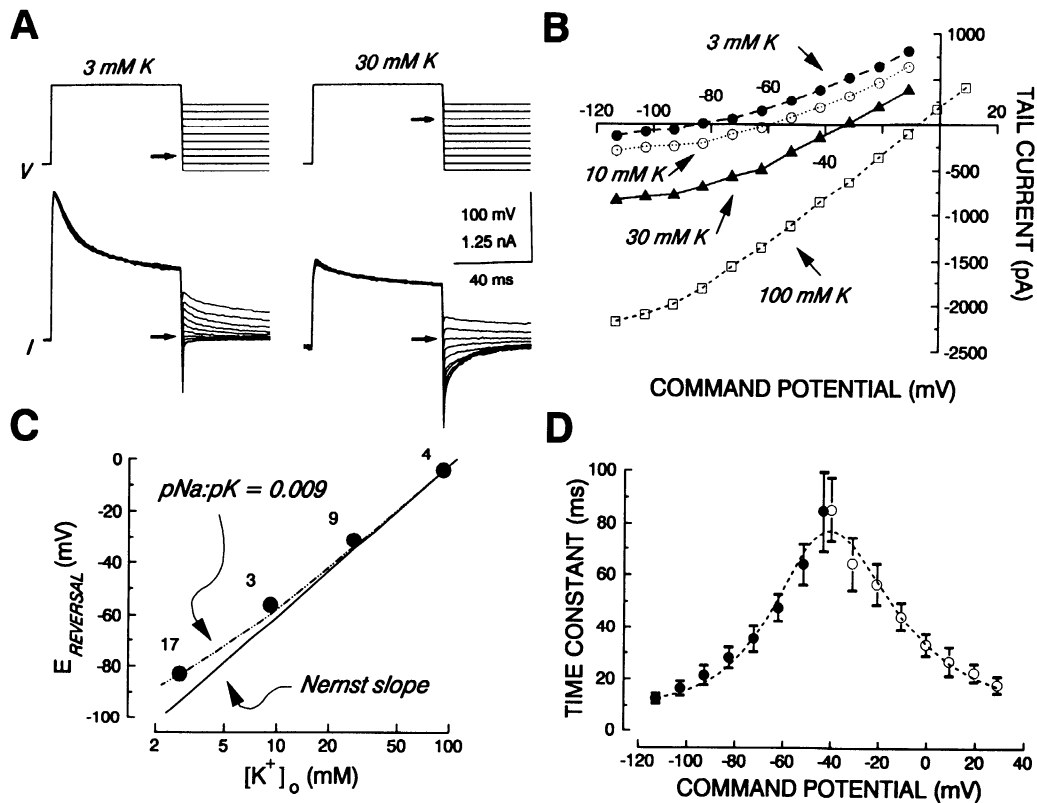


FIG. 4.  $K^+$  dependence and voltage-dependent kinetics of  $I_{K2}$ . *A*: tail currents for  $I_{K2}$  in the presence of 3 and 30 mM  $[K^+]_o$ .  $I_{K2}$  was activated by 100-ms steps to +20 mV from a  $V_{hold}$  of -90 mV. In 3 mM  $K^+$ , tail currents reversed polarity at -82 mV ( $\rightarrow$ ), whereas in 30 mM  $K^+$  reversal occurred at -32 mV. *B*: tail current reversal plots for  $I_{K2}$ , measured in 1 cell with different  $[K^+]_o$ s. *C*: reversal potential dependence for  $I_{K2}$ , measured in several cells.  $[K^+]_o$  is plotted on a semilog axis; numbers above the points indicate number of cells. All standard errors were smaller than symbols. *D*: voltage dependence of activation and deactivation rates. Solid circles ( $n = 8$ ) are average values for time constant of deactivation as measured by tail current decay. Open circles ( $n = 4-10$ ) are values of  $\tau_m$  obtained from Hodgkin-Huxley fitted curves to millimolar-TEA-sensitive current traces. Broken line is an arbitrarily fitted smooth curve.

such subtracted traces, it appears that  $I_{K1}$  activates rapidly (within 10–30 ms, Fig. 2*D*), does not significantly inactivate within 1 s, and rapidly deactivates.

#### $K^+$ dependence of $I_{K2}$

The ionic dependence of  $I_{K2}$  was determined with tail current reversal potential experiments. As previously noted,  $I_{K1}$  decays or deactivates relatively rapidly, so slow tail currents are a means to isolate  $I_{K2}$ . Depolarizations that maximally activated  $I_{K2}$  were applied, followed by return of the membrane potential to a range of voltages above and below the reversal potential. As shown in Fig. 4*A*, this was repeated after changing  $[K^+]_o$ . Reversal potential varied with extracellular  $K^+$  (Fig. 4*B*), the relationship being close to that expected from the Nernst equation (Fig. 4*C*). A small deviation from linearity was observed with the lowest  $[K^+]_o$ , which could be explained by assuming that  $Na^+$  ions are somewhat permeant through  $I_{K2}$  channels. The dashed line in Fig. 4*C* is that expected when  $Na^+$  permeability is 0.9% of  $K^+$  permeability. Replacement of intracellular  $Cl^-$  with gluconate did not affect the reversal potential for  $I_{K2}$  when  $[K^+]_o$  was 3 or 30 mM ( $n = 4$ ), indicating that a chloride conductance does not contribute to the tail currents recorded under these circumstances.

#### Voltage-dependent activation of $I_{K1}$ and $I_{K2}$

The voltage dependence of  $I_{K2}$  activation was examined in two ways. In the first, activation curves were fitted to tail current–command potential plots as in Fig. 5, *A* and *B*. Voltage-clamp commands of sufficient duration (100 ms) to activate peak  $I_{K2}$  were applied to various potentials, and tail current amplitude was measured on termination of the depolarizing step. Using the subtraction technique described above, we isolated  $I_{K2}$  as the current occluded by 20 mM TEA, and we fitted the data in Fig. 5*B* with a Boltzman activation curve of the form

$$g_K = \frac{g_{K,max}}{1 + \exp\left[\frac{(V - V_{1/2})}{k}\right]} \quad (1)$$

where  $V_{1/2}$  is the voltage at which the conductance is one-half maximally activated,  $V$  is the membrane command potential,  $k$  is the slope factor, and  $g_{K,max}$  is the maximum conductance. Conductances were converted to currents by

$$I_K = g_K \times (V - V_K) \quad (2)$$

where  $V_K$  is the  $K^+$  equilibrium potential. Group data for  $I_{K2}$  activation curves are given in Table 1 for the first method. The second experimental approach to investigate activation was to apply least-squares fitting routines of *Eqs.*

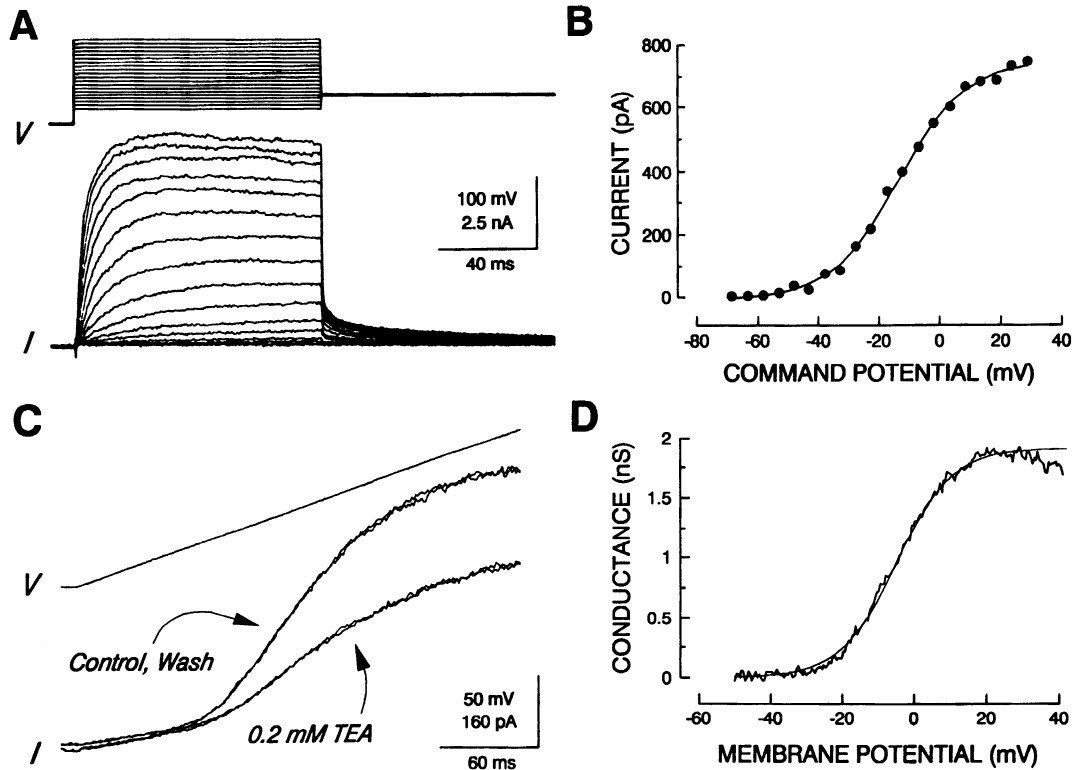


FIG. 5. Voltage-dependent activation of  $I_{K1}$  and  $I_{K2}$ . *A*:  $I_{K2}$  (millimolar-TEA-sensitive current) was activated by step depolarizations to various potentials from a holding potential of  $-90$  mV. At termination of step depolarization, membrane potential was returned to  $-50$  mV, and activation was measured as tail current amplitude at a latency of 12 ms. *B*: activation curve as obtained from tail currents in *A*. Smooth curve is a Boltzmann function with  $k = 11.1$  mV,  $V_{1/2} = -13.7$  mV, and  $I_{max} = 754$  pA. The calculated  $g_{max}$  is 22.9 nS. *C*: currents obtained in response to 300-ms voltage ramps ( $V$ ) from  $-50$  to  $+60$  mV. Bath solution was twice cycled between control and 0.2 mM TEA, and superimposed current responses ( $I$ ) are shown for each cycle. Effects of TEA were completely reversible and repeatable. *D*: activation curve for current blocked by 0.2 mM TEA, normalized for driving force ( $E_K = -83$  mV). The Boltzmann function indicates that  $I_{K1}$  is one-half activated near  $-5$  mV and has a slope factor of 7.8/mV and a maximum conductance of 1.9 nS.

*I* and 2 to current-voltage ( $I$ - $V$ ) plots. Essentially the same results were obtained with the second method. For example, the results of a nonlinear least-squares routine show that the peak currents in Fig. 3C could be well fitted with the following parameters:  $g_{K,max}$ , 56 nS;  $V_K$ ,  $-83$  mV;  $k$ , 8.3 mV $^{-1}$ ; and  $V_{1/2}$ ,  $-10.5$  mV.

Activation of  $I_{K1}$  was assessed by the use of voltage ramps (Fig. 5C). With the holding potential set at  $-50$  mV,  $I_{K2}$  was largely inactivated (see Fig. 6); and, because activation is rapid and inactivation is negligible (with depolarizations to 0 mV,  $I_{K1}$  decayed only  $6.1 \pm 2.3\%$  from peak levels in 600 ms; mean  $\pm$  SE,  $n = 9$ ), this approach allowed for measurement of activation across a large voltage range. The

activation curve (Fig. 5D) is similar to that for  $I_{K2}$  (Fig. 5B; Table 1), the main difference being that the maximum conductance was near 2 nS for  $I_{K1}$  compared with 35 nS for  $I_{K2}$ . We tested pharmacological blockers for specificity against  $I_{K1}$  versus  $I_{K2}$ . One agent, 4-aminopyridine (4-AP), which blocks  $I_A$  in these neurons at millimolar concentrations, also blocks  $I_{K1}$  with an  $IC_{50}$  near 50  $\mu$ M. In the presence of 0.2 mM TEA, 100  $\mu$ M 4-AP produced very little additional current blockade over that obtained in TEA alone ( $n = 4$ ). A component of bee venom, MCD peptide, which is known to block  $K^+$  channels in some systems (Strong 1990), also blocked a small conductance, time-invariant outward current at relatively high concentrations (2  $\mu$ M).

TABLE 1. Activation and inactivation curves for  $I_{K1}$  and  $I_{K2}$

$I_{K1}$ Activation ( $n = 14$ )			$I_{K2}$ Activation ( $n = 15$ )			$I_{K2}$ Inactivation ( $n = 8$ )			
$V_{1/2}$ , mV	$k$ , mV $^{-1}$	$g_{max}$ , nS	$V_{1/2}$ , mV	$k$ , mV $^{-1}$	$g_{max}$ , nS	$V_{1/2}$ , mV	$k$ , mV $^{-1}$	$I_{ss}$ , nA	$I_{nss}$ , nA
$-1.9 \pm 1.3$	$8.6 \pm 0.4$	$2.7 \pm 0.6$	$-12 \pm 2.5$	$12 \pm 0.3$	$36 \pm 3.9$	$-63 \pm 1.5$	$13 \pm 0.5$	$1.8 \pm 0.2$	$0.53 \pm 0.11$

$V_{1/2}$ ,  $k$ , and  $g_{max}$  are values derived from curves fitted to Eqs. 1 and 2. For activation curves,  $I_{K1}$  and  $I_{K2}$  were isolated as in Fig. 5, D and B, respectively. Steady-state inactivation of  $I_{K2}$  (millimolar-TEA-sensitive current) for depolarizations to 0 mV.  $I_{ss}$  refers to amount of current that could be steady-state inactivated through reductions in holding potential, whereas  $I_{nss}$  indicates current that was not steady-state inactivated.  $n$ , number of cells.

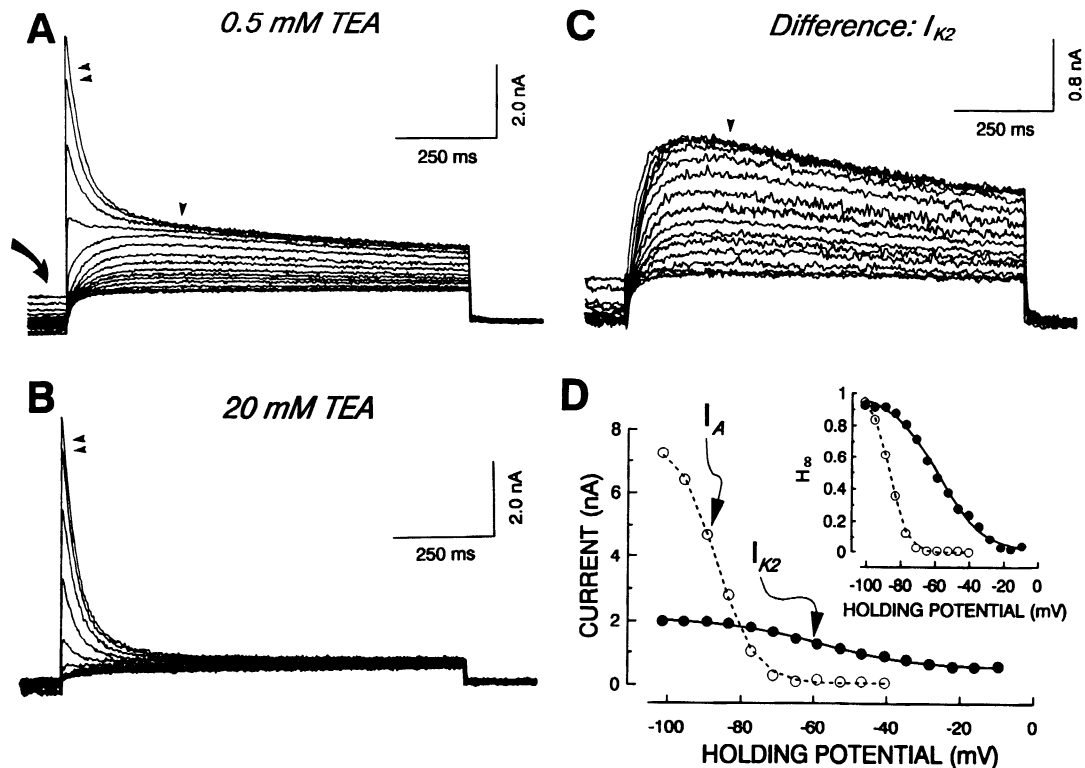


FIG. 6. Steady-state inactivation of  $I_{K2}$ . *A*: currents produced by 1-s steps to 0 mV, which had been preceded by 2-s conditioning steps to various potentials in the range between  $-110$  and  $-10$  mV. Curved arrow indicates currents at conclusion of conditioning step. Largest current was produced by the most hyperpolarized conditioning potential. Note that both the early transient current ( $\blacktriangleleft$ ) and the late current ( $\blacktriangledown$ ) become smaller as the conditioning step is made less negative. *B*: currents produced by same protocol as in *A*, but now in presence of 20 mM TEA. Late current is now nearly independent of conditioning potential. *C*: millimolar-TEA-sensitive current (difference traces from *A* and *B*) exhibits steady-state inactivation. *D*: peak current amplitude for  $I_A$  and  $I_{K2}$ , as obtained from currents in *B* and *C*. Arrows indicate half-inactivating membrane potentials for the 2 components ( $-87$  and  $-59$  mV). Slopes for fitted Boltzman curves were 5.3 and 13.4  $\text{mV}^{-1}$  for  $I_A$  and  $I_{K2}$ , with  $I_{\text{max}}$  values of 7.6 and 1.6 nA, respectively, whereas corresponding noninactivating components were 0 and 0.5 nA. *Inset*: normalized  $h_\infty$  curves for  $I_A$  ( $\circ$ ) and the inactivating portion of  $I_{K2}$  ( $\bullet$ ).

### Ca dependence of $I_{K1}$ and $I_{K2}$

As shown in Fig. 4*D*, the maximum conductance of  $I_{K1}$  decreased with very strong depolarizations. Other voltage ramp experiments indicated that the submillimolar-TEA-sensitive current peaked near  $+30$  mV, became smaller with further depolarizations up to  $+60$  mV, and then became larger again with further depolarization (not shown). Because large depolarizations which approach the calcium equilibrium potential ( $E_{\text{Ca}}$ ) can result in reduced  $\text{Ca}^{2+}$  influx, this finding is consistent with  $I_{K1}$  being at least partially  $\text{Ca}^{2+}$  dependent, even in the presence of intracellular calcium buffering (Marty and Neher 1985). The results of additional experiments performed without the intracellular  $\text{Ca}^{2+}$  buffer, EGTA, provided further support for this conclusion. The amplitude of  $I_{K1}$  was larger in the absence of EGTA ( $1.4 \pm 0.6$  nA at 0 mV,  $n = 4$ ) than in its presence ( $0.2 \pm 0.05$  nA,  $n = 11$ ;  $P < 0.01$ , Student's 2-tailed  $t$  test). In addition, without EGTA,  $I_{K1}$  became larger ( $1.5 \pm 0.1$ -fold increase,  $n = 6$ ) when  $[\text{Ca}^{2+}]_o$  was increased to 3 mM. Furthermore, in contrast to recordings made in the presence of EGTA (e.g., Fig. 2*D*), changes in the holding potential, which are known to increase  $I_{\text{Ca}}$  (Coulter et al. 1989a), caused changes in the amplitude of  $I_{K1}$ . Hyperpolarizing the holding potential from  $-40$  to  $-90$  mV resulted

in a  $1.8 \pm 0.2$ -fold increase in  $I_{K1}$  ( $n = 10$ ) compared with  $1.2 \pm 0.1$  with EGTA ( $n = 9$ ,  $P < 0.01$ ).

However, the results of other experiments indicated that  $I_{K1}$  was not entirely dependent on  $\text{Ca}^{2+}$  entry. The addition of 0.2 mM  $\text{Cd}^{2+}$ , which blocks  $>95\%$  of high-threshold  $\text{Ca}^{2+}$  currents (Coulter et al. 1989a), did not reduce the ability of 0.2 mM TEA to block a time-invariant current ( $n = 3$ ). It is possible that, with sufficient depolarization, resting levels of  $[\text{Ca}^{2+}]_i$  may activate  $I_{K1}$ . Replacement of 1 mM extracellular  $\text{Ca}^{2+}$  by 0.75 mM  $\text{Co}^{2+}$  reduced the depression of  $I_{K1}$  by 0.2 mM TEA when the holding potential ( $V_{\text{hold}}$ ) was  $-90$  mV and abolished the effect with  $V_{\text{hold}}$  of  $-40$  mV ( $n = 4$ ). These effects of  $\text{Co}^{2+}$  replacement for  $\text{Ca}^{2+}$  occurred only when EGTA was absent. One explanation for this finding is that  $\text{Co}^{2+}$  might enter the cell and act as an antagonist at intracellular  $\text{Ca}^{2+}$  binding sites.

Calcium-dependent  $I_K$  did not appear to contribute to  $I_{K2}$ , because the inorganic  $\text{Ca}^{2+}$  channel blocker  $\text{Cd}^{2+}$  (0.2 mM) did not affect maximum conductance ( $110 \pm 9.6\%$  of control,  $n = 6$ ). It did, however, shift the activation in the depolarized direction ( $6.2 \pm 1.4$  mV,  $n = 6$ ), consistent with either a screening charge effect (Frankenhauser and Hodgkin 1957) or modulation by a specific divalent cation binding site (cf. Mayer and Sugiyama 1988). In addition, manipulations that altered  $I_{K1}$ —replacement of  $[\text{Ca}^{2+}]_o$

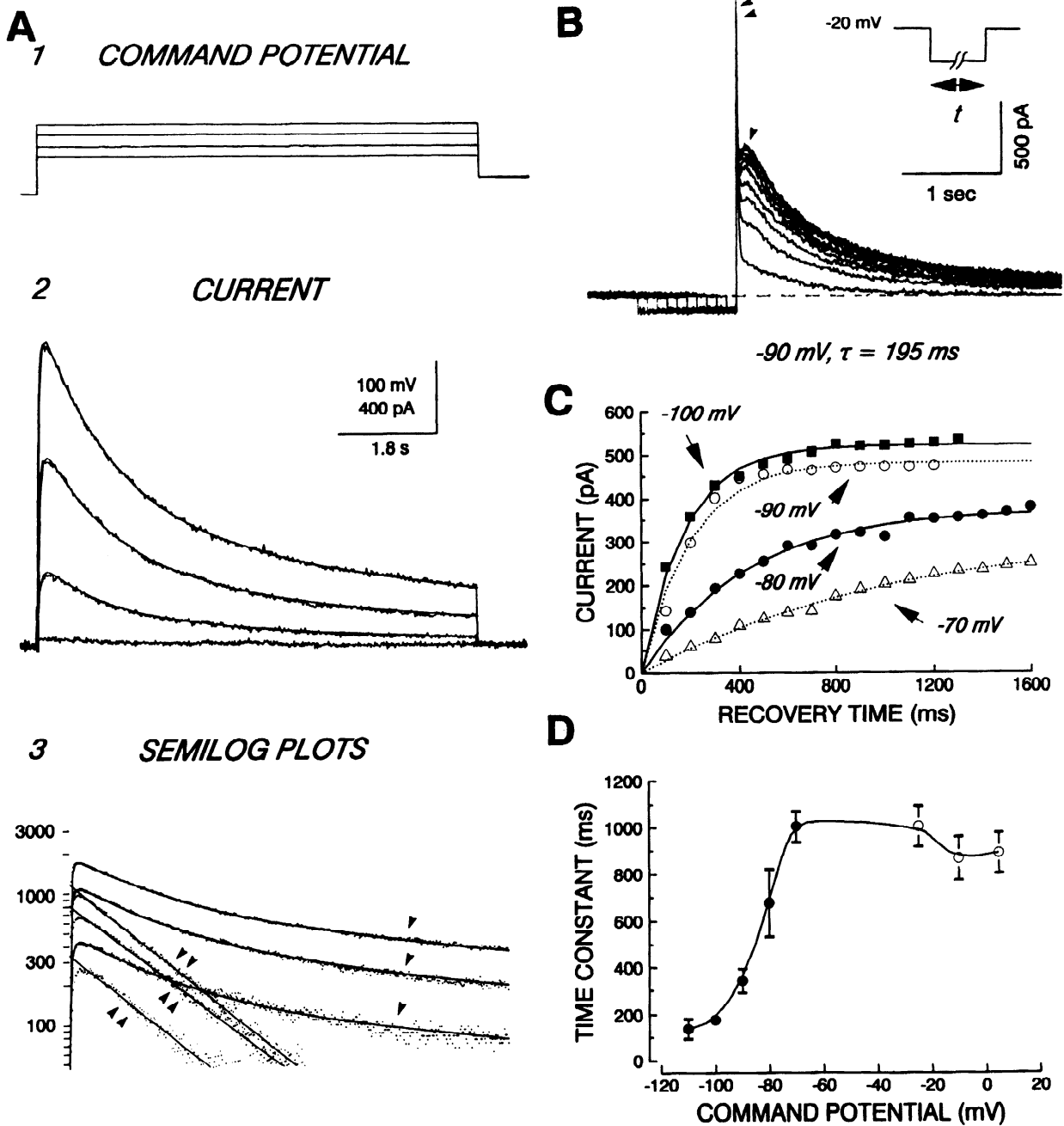


FIG. 7. Inactivation kinetics for  $I_{K2}$ . *A*: millimolar-TEA-sensitive current ( $I_{K2}$ ) was obtained in isolation by subtracting 20 mM from 0.5 mM TEA traces. Long depolarizations (8 s) to -40, -25, -10, and +5 mV were preceded by 1-s conditioning steps to -90 mV. At least 2 traces at each potential were obtained in each concentration of TEA. *I*: command steps for all traces. *2*:  $I_{K2}$  current traces with superimposed fitted curves. *3*: semilog plots for currents obtained with 3 most depolarized potentials. The 3 long, curving traces (single arrowheads) have superimposed fitted curves for a 2-component exponential decay process with time constants near 1 and 10 s (see Table 2). Isolated fast decay components for each trace are shown as steeper sloped, parallel lines marked with double arrowheads. Note that *1*) inactivation of the current is not exponential because the decay, as plotted on semilog axes, is nonlinear; and *2*) the fast rate of decay is voltage-independent, as seen in similar slopes for each line marked with a double arrowhead. *B*: deinactivation of  $I_{K2}$ . Rate of recovery of inactivated current was determined by completely inactivating the current by setting the holding potential to -20 mV and then step hyperpolarizing to -90 mV with increasing durations. Fast transient current ( $I_A$ ) recovers relatively quickly (double arrowhead), whereas the 2nd peak outward current ( $I_{K2}$ ) requires longer conditioning hyperpolarizations to attain maximum amplitude. *C*: recovery of peak  $I_{K2}$  at various potentials, with superimposed fitted curves. Time constants were 1,030, 430, 195, and 175 ms at potentials of -70, -80, -90, and -100 mV, respectively. *D*: voltage dependence for time constant of fast inactivation ( $\circ$ ,  $n = 8$ ) from Hodgkin-Huxley fitted curves and deinactivation ( $\bullet$ ,  $n = 2-11$ ) from fitted recovery curves.

TABLE 2. Time constants of activation and inactivation for  $I_{K2}$ 

Command Potential, mV	$\tau_m$ , ms	$\tau_{h1}$ , s	$\tau_{h2}$ , s	$A_1$ , pA	$A_2$ , pA	$\frac{A_1}{A_1 + A_2}$
Figure 7						
-25	53	1.3	10	348	166	0.68
-10	49	1.4	10	820	417	0.66
+5	42	1.3	10	1,175	762	0.61
Mean $\pm$ SE ( $n = 8$ )						
-25	68 $\pm$ 12	1.0 $\pm$ 0.086	8.4 $\pm$ 0.6	400 $\pm$ 120	280 $\pm$ 93	0.61 $\pm$ 0.05
-10	35 $\pm$ 7.0	0.87 $\pm$ 0.094	8.8 $\pm$ 0.6	1,100 $\pm$ 340	700 $\pm$ 223	0.61 $\pm$ 0.04
+5	19 $\pm$ 5.9	0.89 $\pm$ 0.087	9.6 $\pm$ 0.2	1,600 $\pm$ 480	1,100 $\pm$ 310	0.61 $\pm$ 0.04

Millimolar-TEA-sensitive currents (0.5 mM TEA – 20 mM TEA) were fitted to Eq. 1. Numbers in last column indicate fraction of total current that is rapidly ( $\tau_{h1}$ ) inactivating. Parameters  $\tau_m$ ,  $\tau_{h1}$ ,  $\tau_{h2}$ ,  $A_1$ , and  $A_2$  are defined in Eq. 3.

with  $\text{Co}^{2+}$  ( $n = 3$ ) or increasing  $[\text{Ca}^{2+}]_o$  from 1 to 3 mM ( $n = 5$ )—did not significantly affect the kinetics or amplitude of  $I_{K2}$ .

#### Kinetics of activation and deactivation of $I_{K2}$

Deactivation rate for the millimolar-TEA-sensitive current was obtained by fitting single exponential decays to the tail currents from experiments such as those in Fig. 5A. The rate of decay was found to be independent of  $[\text{K}^+]_o$  but strongly dependent on voltage, with the time constant varying between 10 and 60 ms in the range of membrane potentials between -110 and -50 mV. Activation rate was obtained by fitting a Hodgkin-Huxley type model to  $I_{K2}$  waveforms (e.g., Fig. 7A2). The following model was used

$$I_{K2} = \left[ 1 - \exp\left(-\frac{t}{\tau_m}\right) \right]^N \times \left[ A_1 \exp\left(-\frac{t}{\tau_{h1}}\right) + A_2 \exp\left(-\frac{t}{\tau_{h2}}\right) \right] \quad (3)$$

where  $\tau_m$  is the time constant of activation,  $\tau_{h1}$  and  $\tau_{h2}$  are time constants of inactivation,  $A_1$  and  $A_2$  are amplitudes of the two inactivation components, and  $N$  is a power factor that affects the delay to peak current (Hodgkin and Huxley 1952). Surprisingly, in this preparation, we found that a power factor near 1 best describes the current waveform. This is in contrast to the value of 4, which is assumed for delayed rectifier currents in squid giant axon (Hodgkin and Huxley 1952). The value of  $\tau_m$  was found to vary between 60 and 20 ms in the voltage range of -40 to +30 mV (Fig. 5D).

#### Steady-state inactivation of $I_{K2}$

As described in a previous report and evident in Fig. 2,  $I_{K2}$  undergoes significant steady-state inactivation as the membrane potential is made less hyperpolarized. Figure 6 shows an experiment in which  $I_{K2}$  was isolated and its steady-state inactivation characterized. In 0.5 mM TEA solution, as the conditioning membrane potential was gradually made more depolarized (Fig. 6A), both  $I_A$  and the late outward current became smaller. In the presence of 20 mM TEA, which nearly completely blocks  $I_{K2}$ , only  $I_A$  remains, and the late current amplitude is now independent of conditioning potential (Fig. 6B). The difference currents, displayed at high gain in Fig. 6C, show that  $I_{K2}$  begins to be

come inactivated around -90 mV, and reaches a steady, nonzero level, with conditioning potentials near -20 mV. This steady level, or offset, was observed in all cells, indicating that  $I_{K2}$  does not completely steady-state inactivate (see Table 2). Normalized inactivation ( $h_\infty$ ) curves for  $I_A$  and  $I_{K2}$  (Fig. 6D, inset) show that  $I_{K2}$  inactivates over a broader voltage range and at more depolarized levels than  $I_A$ . Average values for  $I_{K2}$  inactivation are given in Table 1.

#### Inactivation kinetics for $I_{K2}$

Inactivation of  $I_{K2}$  could not be described by a single exponential decay process (Fig. 7A3). Therefore Eq. 3 was used to describe the time course of the current. As previously noted (Figs. 3 and 5), the rate of activation was voltage dependent. In contrast, inactivation rate was relatively independent of voltage. The current traces in Fig. 7, A1 and A2, are shown with curves drawn to Eq. 3 superimposed. The fitting parameters are given in Table 2. At each potential, two time constants with values of  $\sim 1$  and 10 s were necessary to describe the current decay. Group data for  $I_{K2}$  current decay are given in Table 2. The fast inactivation rate at depolarized potentials was insensitive to voltage (Fig. 7D).

Deinactivation, or recovery from inactivation, was studied by the use of the protocol shown in Fig. 7B, inset. As the duration of the conditioning hyperpolarization was increased, the amplitudes of both  $I_A$  and  $I_{K2}$  became larger. The rates of deinactivation in a single cell (Fig. 7C) and in the population of cells (Fig. 7D) show that the deinactivation time constant was voltage dependent, increasing from <200 ms at -110 mV to >1 s at -70 mV. In the presence of 20 mM TEA, the late peaking current was completely abolished, so there was no need for pharmacological subtraction with the deinactivation protocol.

#### Temperature dependence of $I_{K2}$

Because other voltage-dependent currents in RNs are known to vary significantly with temperature ( $I_T$ , Coulter et al. 1989a;  $I_A$ , Huguenard et al. 1991), we analyzed the kinetics and amplitude of  $I_{K2}$  as bath temperature was changed from the usual recording temperature of  $\sim 22^\circ\text{C}$  to warmer values. In the first of two experimental ap-

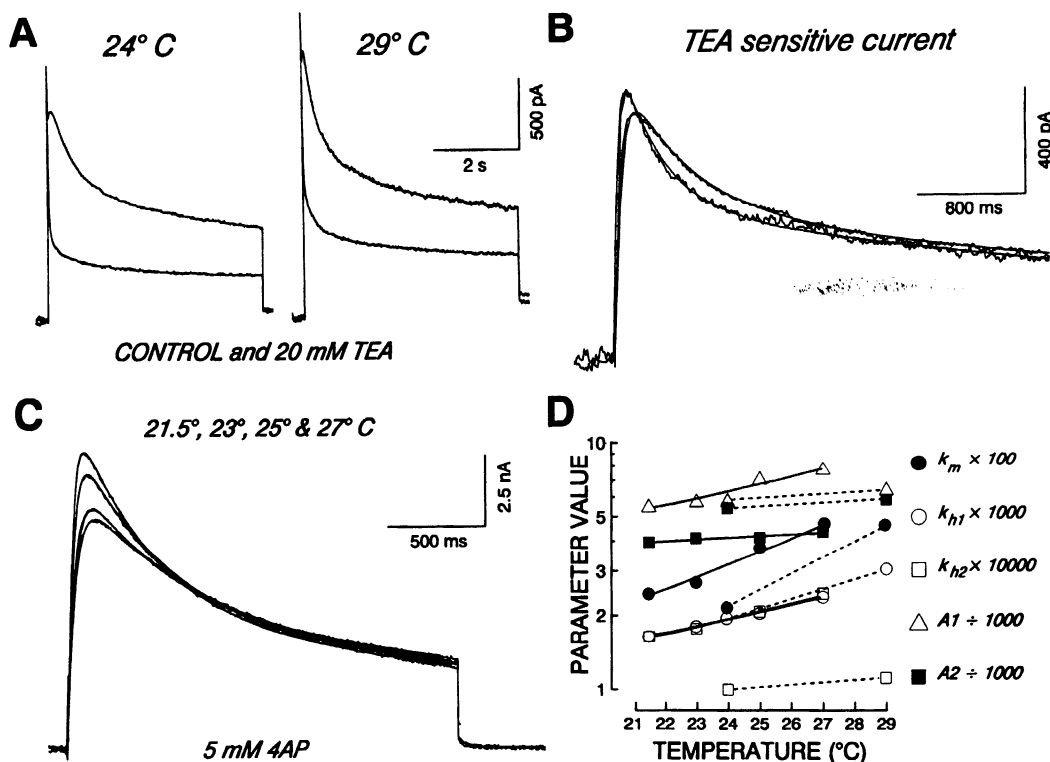


FIG. 8. Temperature dependence of  $I_{K2}$ . *A*: currents obtained with depolarization to 0 from  $-90$  mV, in control and in presence of 20 mM TEA, at 24 and 29°C. *B*: TEA-sensitive currents with overlaid fitted Hodgkin-Huxley curves. *C*: currents and fitted curves, obtained with same voltage protocol as in *A*, but in presence of 5 mM 4-AP to block  $I_A$ . As temperature was increased, activation and inactivation of  $I_{K2}$  became faster and current amplitude increased. *D*: group data for temperature dependence of  $I_{K2}$ . Solid lines are those from the 4-AP experiment in *C*, whereas dashed lines are the TEA-sensitive current from *B*. Kinetic parameters are represented as rate constants ( $k$ ), which are reciprocal time constants. All parameters are as defined for Eq. 3. Note that  $A_2$  (■) is considerably less temperature sensitive (has a flatter slope) than the other parameters.  $A_1$  and  $A_2$  are in units of picoamperes, whereas  $k_m$ ,  $k_{h1}$ , and  $k_{h2}$  are in units of reciprocal milliseconds.

proaches, the millimolar-TEA-sensitive current was obtained by subtraction at multiple temperatures (Fig. 8, *A* and *B*); in the second,  $I_A$  was blocked by 5 mM 4-AP (Fig. 8*C*), and the remaining current was assumed to be largely due to  $I_{K2}$ . The total current in the presence of 4-AP was kinetically analyzed as a function of temperature (Fig. 8*D*). In both types of experiments, the rate constants and amplitudes were found to increase with temperature (Fig. 8*D*). The temperature coefficients ( $Q_{10}$ s) for group data are given in Table 3.

DISCUSSION

Our results in isolated RNs show that, in addition to  $I_A$ , there are at least two depolarization-activated  $K^+$  conductances,  $I_{K2}$  and  $I_{K1}$ , which have either slow or negligible inactivation and which are both blocked by extracellular TEA. These currents can be isolated on the basis of their differential TEA sensitivity. At a concentration of 0.2 mM, TEA blocks  $\sim 87\%$  of  $I_{K1}$  (Huguenard et al. 1991) while

inhibiting  $I_{K2}$  by only 5%. Therefore the difference in currents between control and 0.2 mM TEA conditions is almost entirely due to  $I_{K1}$ . Because 0.5 mM TEA blocks 95% of  $I_{K1}$  and 11% of  $I_{K2}$ , whereas 20 mM TEA blocks 84% of  $I_{K2}$ , the difference currents obtained from the latter subtraction (0.5 mM TEA – 20 mM TEA) are an effective means to isolate  $I_{K2}$ . The use of pharmacological tools has thus allowed us to perform a kinetic analysis of these two relatively long-lasting, depolarization-activated  $K^+$  currents.

With an average underlying conductance of 36 nS,  $I_{K2}$  is the predominant late outward current in VB neurons. Given an average membrane capacitance of 17.5 pF for acutely isolated RNs (Huguenard et al. 1991), the resulting normalized conductance is near 2 nS/pF, or 20 pS/ $\mu m^2$ , assuming a specific membrane capacitance of 1  $\mu F/cm^2$ . By contrast,  $I_{K1}$  averaged only 2.7 nS, giving values of 0.15 nS/pF and 1.5 pS/ $\mu m^2$ .

Properties of  $I_{K1}$

Intracellular voltage recordings from guinea pig thalamic relay neurons provided evidence for a  $Ca^{2+}$ -dependent single-spike afterhyperpolarization, which was blocked by  $Co^{2+}$  and  $Mg^{2+}$  replacement for  $Ca^{2+}$  (Jahnsen and Llinás 1984). Several lines of evidence point to  $I_{K1}$  as being a

TABLE 3. Temperature coefficients,  $I_{K2}$  kinetics, and amplitude

$\tau_m$	$\tau_{h1}$	$\tau_{h2}$	$A_1$	$A_2$
$2.9 \pm 0.8$	$2.6 \pm 0.4$	$2.6 \pm 0.6$	$1.9 \pm 0.2$	$1.1 \pm 0.1$

$n = 4$  cells. Abbreviations, see Eq. 3.

$\text{Ca}^{2+}$ -dependent current that could contribute to such afterhyperpolarizations. First of all, the current is relatively small (0.2 nA at 0 mV) when intracellular calcium is highly buffered with 10 mM EGTA, which results in a calculated free  $[\text{Ca}^{2+}]_i$  of <10 nM. When EGTA was not present,  $I_{K1}$  was much larger, and was apparently sensitive to the amount of  $\text{Ca}^{2+}$  entry that occurred during the depolarization. Increasing  $I_{Ca}$  either by raising  $[\text{Ca}^{2+}]_o$  or by making the conditioning pulse more hyperpolarized (Coulter et al. 1989a) increased the amplitude of  $I_{K1}$ . In addition, the submillimolar TEA sensitivity of  $I_{K1}$  resembles that of the fast,  $\text{Ca}^{2+}$ -sensitive afterhyperpolarization in rat hippocampal neurons (Lancaster and Nicoll 1987), of  $\text{Ca}^{2+}$ -activated SK channels in GH<sub>3</sub> cells (Lang and Ritchie 1990), of the fast  $\text{Ca}^{2+}$ -dependent  $\text{K}^+$  current ( $I_C$ ) in frog sympathetic neurons (Pennefather et al. 1985), and of the  $\text{Ca}^{2+}$ -dependent but EGTA-resistant  $\text{K}^+$  current in adrenal chromaffin cells (Marty and Neher 1985). The failure of the inorganic Ca-current blocker,  $\text{Cd}^{2+}$ , to reduce  $I_{K1}$  (i.e., the current blocked by 0.2 mM TEA), even in the presence of intracellular EGTA, does not necessarily rule out a Ca-activated component of  $I_{K1}$ . This latter finding may be explained by voltage-dependent activation of  $I_{K1}$  at relatively low resting levels of  $[\text{Ca}^{2+}]_i$ , which would be independent of  $\text{Ca}^{2+}$  entry. Alternatively, 0.2 mM  $\text{Cd}^{2+}$  blocks only 97% of  $I_{Ca}$ , and the remaining fractional current might produce sufficient increases of  $[\text{Ca}^{2+}]_i$  to activate  $I_{K1}$ . With  $\text{Co}^{2+}$  substitution for  $\text{Ca}^{2+}$ , however,  $I_{K1}$  was blocked.

The activation and deactivation kinetics of  $I_{K1}$  are relatively fast compared with those of  $I_{K2}$ . At 0 mV, peak amplitude of  $I_{K1}$  was normally attained in <30 ms; and, on termination of a depolarizing command step,  $I_{K1}$  rapidly decayed to baseline current (Fig. 2D).  $I_{K1}$  is not steady-state inactivated, nor does it markedly decay during maintained depolarization, when EGTA is included in the pipette. The threshold for activation is near -30 mV, and peak current is attained near +20 mV. Because  $I_{K1}$  was obtained by subtraction in the presence of another much larger current ( $I_{K2}$ ) that could not be selectively blocked, the activation and inactivation kinetics and the steady-state inactivation could not be determined with greater precision than that presented here. However, it appears that  $I_{K1}$  activates rapidly enough to contribute to single action potential repolarization.

#### Properties of $I_{K2}$

The kinetics of  $I_{K2}$  activation and deactivation were much slower than those of  $I_{K1}$ . At room temperature,  $I_{K2}$  activated with a threshold near -40 mV, and peak current was attained with a latency between 50 and 500 ms from the onset of the depolarizing voltage-clamp command step (Fig. 3D). After reaching peak amplitude,  $I_{K2}$  decayed slowly over a period of several seconds (Figs. 3 and 6-8). These kinetics would result in a gradual depolarization in current-clamp recordings as  $I_{K2}$  inactivated during maintained current injections with eventual approach to spike threshold, as seen in Fig. 1 (and also in Fig. 10 of Jahnsen and Llinás 1984). With maintained depolarization, further inactivation of  $I_{K2}$  would contribute to accelerated spike firing. A similar action is seen in neurons of the hippocam-

pus (Storm 1988), inferior olive (Yarom and Llinás 1987), cat sensorimotor cortex (Spain et al. 1991), hypothalamus (Greene et al. 1990), and vagal motor nucleus (Laiwand et al. 1988). A notable difference between  $I_{K2}$  and the slowly inactivating outward currents seen in hippocampus and neocortex is a reduction of the latter by low concentrations of 4-AP (<1 mM) and an insensitivity to TEA blockade, which contrasts markedly with the pharmacology of  $I_{K2}$  in RNs. In addition, the threshold for  $I_{K2}$  activation is somewhat more depolarized than that for the slow transient current seen in these other types of neurons.

Although several properties (e.g., voltage dependence and millimolar TEA sensitivity) of  $I_{K2}$  resemble those of the delayed rectifier current in axons (Hodgkin and Huxley 1952) and invertebrate neurons (Aldrich et al. 1979; Connor and Stevens 1971a),  $I_{K2}$  is not likely to contribute to rapid action potential repolarization. Because  $I_A$  and  $I_{K1}$  both activate with much faster kinetics, these latter currents are presumably largely responsible for the falling phase of single action potentials.

Activation of  $I_{K2}$  resembles that observed for  $\text{K}^+$  currents in other central mammalian neurons. In guinea pig hippocampal neurons (Sah et al. 1988),  $I_K$  is one-half activated at -5 mV (compared with -12 mV for  $I_{K2}$ ), with a slope factor of 14 mV<sup>-1</sup> (compared with 12 mV<sup>-1</sup> for  $I_{K2}$ ). However, the rate of  $I_K$  activation in hippocampus is much faster than for  $I_{K2}$  in RNs, with  $\tau_m$  equal to 2 ms at 0 mV in the former, compared with  $\tau_m$  of 30 ms for  $I_{K2}$ . In comparison with  $I_{K2}$ , a power factor of 1 was also found to fit  $I_K$  activation in isolated hippocampal neurons (Sah et al. 1988).

An important feature of  $I_{K2}$  is its steady-state inactivation, a property shared by a variety of  $\text{K}^+$  currents in neurons acutely isolated from rat (Sah et al. 1988) and guinea pig (Numann et al. 1987) hippocampus, as well as those from rat hippocampal cultures (Segal and Barker 1984) and in vitro neocortical slices from cat (Spain et al. 1991). Similar inactivation properties also occur in molluscan neurons (Aldrich et al. 1979; Connor and Stevens 1971a) and squid axons (Clay 1989; Ehrenstein and Gilbert 1966). Because of this steady-state inactivation, RNs have only 50% of the total  $I_{K2}$  available at resting membrane potentials near -60 mV (Fig. 6). In addition, membrane potential changes over a wide range will affect the availability of this channel, one consequence being that steady depolarizations will gradually increase the excitability of these cells. In each of the studies cited above, inactivation of  $I_K$  occurs over a period of seconds, and the rate of inactivation is relatively insensitive to voltage, findings similar to those for  $I_{K2}$  in RNs. We found that  $I_{K2}$  inactivates with two time constants, one near 1 s and another near 10 s, at room temperature. The rates of both the underlying processes had positive values of  $Q_{10}$ ; however, the contribution of the slower process to the total current was diminished by increasing temperatures.

The apparent inactivation of whole-cell  $I_{K2}$  could be the result of voltage-dependent inactivation of individual channels or, alternatively, could be due to delayed opening of channels. In the latter case, macroscopic current inactivation would reflect the activation process in a manner analogous to that described for  $\text{Na}^+$  channels (Aldrich et al.

1983). This is probably the case for  $I_{K2}$ , because it steady-state inactivates and the inactivation rate is relatively voltage independent.

In contrast to inactivation, recovery from inactivation was highly voltage dependent in a manner similar to that reported previously in axons (Clay 1989) and hippocampal neurons (Numann et al. 1987). Therefore, although  $I_{K2}$  can be markedly inactivated by resting potentials near  $-60$  mV, it can rapidly deactivate during hyperpolarizing voltage excursions near  $-80$  mV, which occur with normal membrane oscillations in RNs during functional states (Steriade and Llinás 1988).

#### Functional implications of $I_{K1}$ and $I_{K2}$

Clearly, RNs have integrative functions in the time domain of seconds in addition to the monosynaptic relay of phasic information. This gives neurons the opportunity to sum and respond to tonically occurring subthreshold inputs; i.e., although near-threshold synaptic input does not initially affect output, it does produce a "memory" through slow inactivation of  $I_{K2}$ . When threshold is reached, spike output might reflect a sustained input that began seconds earlier. By contrast, when RNs are relatively hyperpolarized,  $I_{K2}$  is largely available for activation. This may contribute to the postburst pause in firing that occurs during maintained depolarizations that initially produce a  $Ca^{2+}$ -dependent burst of spikes.

Various  $K^+$  currents are known to be a target for neurotransmitter modulation. For example, in hippocampus, a slow afterhyperpolarizing potential (AHP) is blocked by various neuromodulators, including norepinephrine, histamine, acetylcholine, and serotonin (reviewed by Nicoll 1988). RNs are largely devoid of the slow AHP (Jahnsen and Llinás 1984), but there is evidence in squid axons that the delayed rectifier can be modulated by phosphorylation, such that both gating and availability of channels are affected (Augustine and Bezanilla 1990). If  $I_{K2}$  is similarly affected, it would then present a site for neuromodulatory action in RNs.

We thank I. Mody and T. Otis for advice pertaining to obtaining whole-cell recordings in brain slices and E. Brooks and I. Parada for expert technical assistance.

This work was supported by National Institute of Neurological Disorders and Stroke Grants NS-06477, NS-12151, and NS-07280 and the Morris and Pimley Research Funds.

Address for reprint requests: J. R. Huguenard, Dept. of Neurology and Neurological Sciences, Rm. M016 Medical Center, Stanford, CA 94305.

Received 20 March 1991; accepted in final form 4 June 1991.

#### REFERENCES

- ALDRICH, R. W., COREY, D. P., AND STEVENS, C. F. A reinterpretation of mammalian sodium channel gating based on single channel recording. *Nature Lond.* 306: 436-441, 1983.
- ALDRICH, R. W., GETTING, P. A., AND THOMPSON, S. H. Inactivation of delayed outward current in molluscan neurone somata. *J. Physiol. Lond.* 291: 507-530, 1979.
- AUGUSTINE, C. K. AND BEZANILLA, F. Phosphorylation modulates potassium conductance and gating current of perfused giant axons of squid. *J. Gen. Physiol.* 95: 245-271, 1990.
- BLANTON, M. G., LO TURCO, J. J., AND KRIEGSTEIN, A. R. Whole cell recording from neurons in slices of reptilian and mammalian cerebral cortex. *J. Neurosci. Methods* 30: 203-210, 1989.
- BUZSÁKI, G., SMITH, A., BERGER, S., FISHER, L. J., AND GAGE, F. H. Petit mal epilepsy and Parkinsonian tremor: hypothesis of a common pacemaker. *Neuroscience* 36: 1-14, 1990.
- CLAY, J. R. Slow inactivation and reactivation of the  $K^+$  channel in squid axons. A tail current analysis. *Biophys. J.* 55: 407-414, 1989.
- CONNOR, J. A. AND STEVENS, C. F. Inward and delayed outward membrane currents in isolated neural somata under voltage clamp. *J. Physiol. Lond.* 213: 1-19, 1971a.
- CONNOR, J. A. AND STEVENS, C. F. Prediction of repetitive firing behaviour from voltage clamp data on an isolated neurone soma. *J. Physiol. Lond.* 213: 31-53, 1971b.
- COULTER, D. A., HUGUENARD, J. R., AND PRINCE, D. A. Calcium currents in rat thalamocortical relay neurones: kinetic properties of the transient, low-threshold current. *J. Physiol. Lond.* 414: 587-604, 1989a.
- COULTER, D. A., HUGUENARD, J. R., AND PRINCE, D. A. Specific petit mal anticonvulsants reduce calcium currents in thalamic neurons. *Neurosci. Lett.* 98: 74-78, 1989b.
- COULTER, D. A., HUGUENARD, J. R., AND PRINCE, D. A. Differential effects of petit mal anticonvulsants and convulsants on thalamic neurones: calcium current reduction. *Br. J. Pharmacol.* 100: 800-806, 1990.
- CRUNELLI, V., LIGHTOWLER, S., AND POLLARD, C. A T type calcium current underlies the low threshold calcium potential in cells of the cat and rat lateral geniculate nucleus. *J. Physiol. Lond.* 413: 543-561, 1989.
- DESCHÊNES, M., ROY, J. P., AND STERIADE, M. Thalamic bursting mechanism: an inward slow current revealed by membrane hyperpolarization. *Brain Res.* 239: 289-293, 1982.
- EHRENSTEIN, G. AND GILBERT, D. L. Slow changes of potassium permeability in the squid giant axon. *Biophys. J.* 6: 553-566, 1966.
- FRANKENHAEUSER, B. AND HODGKIN, A. L. The action of calcium on the electrical properties of squid axons. *J. Physiol. Lond.* 137: 218-244, 1957.
- GLOOR, P. AND FARIELLO, R. G. Generalized epilepsy: some of its cellular mechanisms differ from those of focal epilepsy. *Trends Neurosci.* 11: 63-68, 1988.
- GREENE, R. W., HAAS, H. L., AND REINER, P. B. Two transient outward currents in histamine neurones of the rat hypothalamus in vitro. *J. Physiol. Lond.* 420: 149-163, 1990.
- HAGIWARA, S. AND OHMORI, H. Studies of calcium channels in rat clonal pituitary cells with patch electrode voltage clamp. *J. Physiol. Lond.* 331: 232-252, 1982.
- HAMILL, O. P., MARTY, A., NEHER, E., SAKMANN, B., AND SIGWORTH, F. J. Improved patch-clamp techniques for high-resolution current recording from cells and cell-free membrane patches. *Pflugers Arch.* 391: 85-100, 1981.
- HERNÁNDEZ-CRUZ, A. AND PAPE, H.-C. Identification of two calcium currents in acutely dissociated neurons from the rat lateral geniculate nucleus. *J. Neurophysiol.* 61: 1270-1283, 1989.
- HODGKIN, A. L. AND HUXLEY, A. F. A quantitative description of membrane current and its application to conduction and excitation in nerve. *J. Physiol. Lond.* 117: 500-544, 1952.
- HUGUENARD, J. R., COULTER, D. A., AND PRINCE, D. A. Whole-cell clamp of rat thalamic neurons reveal two distinct transient K currents. *Soc. Neurosci. Abstr.* 16: 507, 1990.
- HUGUENARD, J. R., COULTER, D. A., AND PRINCE, D. A. A fast transient potassium current in thalamic relay neurons: kinetics of activation and inactivation. *J. Neurophysiol.* 66: 1304-1315, 1991.
- JAHNSEN, H. AND LLINÁS, R. Ionic basis for the electroresponsiveness and oscillatory properties of guinea-pig thalamic neurones in vitro. *J. Physiol. Lond.* 349: 227-247, 1984.
- KAY, A. R. AND WONG, R. K. S. Isolation of neurons suitable for patch-clamping from adult mammalian central nervous systems. *J. Neurosci. Methods* 16: 227-238, 1986.
- LAIWAND, R., WERMAN, R., AND YAROM, Y. Electrophysiology of degenerating neurones in the vagal motor nucleus of the guinea-pig following axotomy. *J. Physiol. Lond.* 404: 749-766, 1988.
- LANCASTER, B. AND NICOLL, R. A. Properties of two calcium-activated hyperpolarizations in rat hippocampal neurons. *J. Physiol. Lond.* 389: 187-203, 1987.
- LANG, D. G. AND RITCHIE, A. K. Tetraethylammonium blockade of apamin-sensitive and insensitive  $Ca^{2+}$ -activated  $K^+$  channels in a pituitary cell line. *J. Physiol. Lond.* 425: 117-132, 1990.
- LLINÁS, R. R. The intrinsic electrophysiological properties of mamma-

- lian neurons: insights into central nervous system function. *Science Wash. DC* 242: 1564-1664, 1988.
- LLINÁS, R. AND JAHNSEN, H. Electrophysiology of mammalian thalamic neurones in vitro. *Nature Lond.* 297: 406-408, 1982.
- MARTY, A. AND NEHER, E. Potassium channels in cultured bovine adrenal chromaffin cells. *J. Physiol. Lond.* 367: 117-141, 1985.
- MAYER, M. L. AND SUGIYAMA, K. A modulatory action of divalent cations on transient outward current in cultured rat sensory neurones. *J. Physiol. Lond.* 396: 417-433, 1988.
- MCCORMICK, D. A. Possible ionic basis for lagged visual responses in cat LGNd relay neurons. *Soc. Neurosci. Abstr.* 16: 159, 1990.
- NICOLL, R. A. The coupling of neurotransmitter receptors to ion channels in the brain. *Science Wash. DC* 241: 545-551, 1988.
- NUMANN, R. E., WADMAN, W. J., AND WONG, R. K. S. Outward currents of single hippocampal cells obtained from the adult guinea-pig. *J. Physiol. Lond.* 393: 331-353, 1987.
- OTIS, T. S., STALEY, K. J., AND MODY, I. Inhibitory activity in mammalian brain slices generated by spontaneous release. *Brain Res.* 545: 142-150, 1991.
- PENNEFATHER, P., LANCASTER, B., ADAMS, P., AND NICOLL, R. A. Two distinct Ca-dependent K currents in bullfrog sympathetic ganglion cells. *Proc. Natl. Acad. Sci. USA* 82: 3040-3044, 1985.
- SAH, P., GIBB, A. J., AND GAGE, P. W. Potassium current activated by depolarization of dissociated neurons from adult guinea pig hippocampus. *J. Gen. Physiol.* 92: 263-278, 1988.
- SEGAL, M. AND BARKER, J. L. Rat hippocampal neurons in culture: potassium conductances. *J. Neurophysiol.* 51: 1409-1433, 1984.
- SEGAL, M., ROGAWSKI, M. A., AND BARKER, J. L. A transient potassium conductance regulates the excitability of cultured hippocampal and spinal neurons. *J. Neurosci.* 4: 604-609, 1984.
- SPAIN, W. J., SCHWINDT, P. C., AND CRILL, W. E. Two transient potassium currents in layer V pyramidal neurones from cat sensorimotor cortex. *J. Physiol. Lond.* 434: 591-607, 1991.
- STERIADE, M. AND LLINÁS, R. R. The functional states of the thalamus and the associated neuronal interplay. *Physiol. Rev.* 68: 649-742, 1988.
- STORM, J. F. Temporal integration by a slowly inactivating K<sup>+</sup> current in hippocampal neurons. *Nature Lond.* 336: 379-381, 1988.
- STRONG, P. N. Potassium channel toxins. *Pharmacol. Ther.* 46: 137-162, 1990.
- SUZUKI, S. AND ROGAWSKI, M. A. T-type calcium channels mediate the transition between tonic and phasic firing in thalamic neurons. *Proc. Natl. Acad. Sci. USA* 86: 7228-7232, 1989.
- VERGNES, M., MARESCAUX, C., AND DEPAULIS, A. Mapping of spontaneous spike and wave discharges in Wistar rats with genetic generalized non-convulsive epilepsy. *Brain Res.* 523: 87-91, 1990.
- YAROM, Y. AND LLINÁS, R. Long-term modifiability of anomalous and delayed rectification in guinea pig inferior olivary neurons. *J. Neurosci.* 7: 1166-1177, 1987.